



Motion blur detection in aerial images shot with channel-dependent exposure time

Lâmân Lelégard, Mathieu Brédif, Bruno Vallet, Didier Boldo

► To cite this version:

Lâmân Lelégard, Mathieu Brédif, Bruno Vallet, Didier Boldo. Motion blur detection in aerial images shot with channel-dependent exposure time. Symposium on Photogrammetric Computer Vision and Image Analysis (PCV), Sep 2010, Saint-Mandé, France. pp.180 - 185. hal-01883139

HAL Id: hal-01883139

<https://hal.science/hal-01883139>

Submitted on 2 Oct 2018

HAL is a multi-disciplinary open access archive for the deposit and dissemination of scientific research documents, whether they are published or not. The documents may come from teaching and research institutions in France or abroad, or from public or private research centers.

L'archive ouverte pluridisciplinaire **HAL**, est destinée au dépôt et à la diffusion de documents scientifiques de niveau recherche, publiés ou non, émanant des établissements d'enseignement et de recherche français ou étrangers, des laboratoires publics ou privés.

MOTION BLUR DETECTION IN AERIAL IMAGES SHOT WITH CHANNEL-DEPENDENT EXPOSURE TIME

L. Lelégard ^{a,*}, M. Brédif ^a, B. Vallet ^a, D. Boldo ^b

^a Université Paris Est, IGN, Laboratoire MATIS, 73 avenue de Paris, 94165 Saint-Mandé, France
(laman.lelegard, mathieu.bredif, bruno.vallet)@ign.fr

^b EDF R&D – Département STEP, 6 quai Watier, 78401 Chatou, France – didier.boldo@edf.fr

Commission III

KEY WORDS: Motion blur, blur detection, airborne imagery, Fourier Transform

ABSTRACT:

This paper presents a simple yet efficient approach for automatic blur detection in aerial images provided by a multi-channel digital camera system. The blur in consideration is due to the airplane motion and causes anisotropy in the Fourier Transform of the image. This anisotropy can be detected and estimated to recover the characteristics of the motion blur, but one cannot disambiguate the anisotropy produced by a motion blur from the possible spectral anisotropy of the underlying sharp image. The proposed approach uses a camera with channel-dependent exposure times to address this issue. Under this multi-exposure setting, the motion blur kernel is scaled proportionally to the exposure-time, whereas the phase differences between the underlying sharp colour channels are assumedly negligible. We show that considering the phase of the ratio of the Fourier Transforms of two channels enhances blur detection. Results obtained on 2000 images confirm the operational efficiency of our method.

1. INTRODUCTION

For more than fifteen years, mapping agencies and photogrammetric companies have been working on digital airborne image acquisition, phasing out traditional silver film. This important change brought many improvements, especially in the radiometric quality of images where each pixel could be given a physical value after a radiometric calibration of the camera, which was not the case with silver film. The chemical process of film development cannot be entirely under control. A good radiometric quality is often required in order to produce ortho-images (i.e. mosaics of images that can be geometrically superposed with a map) without visible boundaries (Kasser & Egels, 2002).

To provide high quality images, the flights often take place in summer, when the brightness is optimal. However flying in summer has one drawback: the significant tree foliage causes problematic occlusions when studying the characteristics of the ground level (topography, path, rivers, etc.). The only way to have leafless trees is to fly the mission between autumn and spring when the luminosity is weak. Thus, the exposure time should be increased, at the risk of causing motion blur. Fortunately, the images in which the blur is significant (more than 2 pixels) represent a very small proportion of the mission.

In preparation for photogrammetric and remote sensing studies, aerial acquisitions are planned with an important overlap between two images. The strong overlaps generally chosen ensure that a ground point appears on at least four pictures. This redundancy is the reason why it can be chosen to simply remove blurred images without trying any restoration. This choice is justified by the fact that it is almost impossible to have all the images seeing the same ground point blurred. Until now the

removal of blurred images was done manually by an operator. We propose in this article an automatic method for blur detection that makes this long and tedious work easier.

First, we will describe the channel-dependent exposure time camera for which our method is designed. Then we will review the state of the art, which will show that blur detection is less discussed than blur correction. Our method of blur detection will then be presented in two parts: first, a simple and mono-channel approach based on the module of the Fourier Transform of the image, then an improvement based on a multi-channel approach. A test on 2000 images eventually illustrates the reliability of the method.

2. DATA ACQUISITION

The images are provided by a multi-channel camera system (Figure 1). This multi-sensor system has been preferred to a classical Bayer sensor for many reasons. Among them, the lack of coloured artefacts, a better dynamic range in the shadowed areas and the possibility of using a fourth channel in the near infra-red wavelengths for remote sensing applications. In our study, only the visible wavelengths (between 380 and 780 nm) are considered.

The relative response of the three channels (R, G, B) are influenced by the KAF-16801LE sensor performances (Eastman Kodak Company, 2002) and by the colour filter transmission (CAMNU, 2005) as illustrated on Figure 2. In particular, the response in the blue channel is very low relative to other channels. There are two solutions to deal with this problem. The first idea is to simply multiply the blue signal by a constant to enhance the blue channel, but its noise will be multiplied

* Corresponding author.

accordingly. This is the solution used in most Bayer sensors, because their exposure time is the same for all the channels. But the designers of the system that we present considered the possibility of physically separating the three colour channels on three independent sensors (Thom et al., 2001). This choice yields the possibility of enhancing the blue signal by augmenting the exposure time which ensures a good signal to noise ratio (SNR) along with a better dynamic range in the blue channel. This is for instance useful in the shadowed areas.

Conversely, for highly luminous scenes, the response in the red channel is very high, such that it may cause sensor saturation, even for small exposure times (Figure 2). To avoid this, another correction, has been brought to the red camera by reducing its aperture. The following table summarises the specificities of the airborne camera system that provided the data exploited in this study:

| Channel | Red | Green | Blue |
|---------------|--------|---------|---------|
| Aperture | f/8,0 | f/5,6 | f/5,6 |
| Exposure time | 8,0 ms | 15,2 ms | 28,0 ms |

Table 1. Aperture and exposure time for each channel

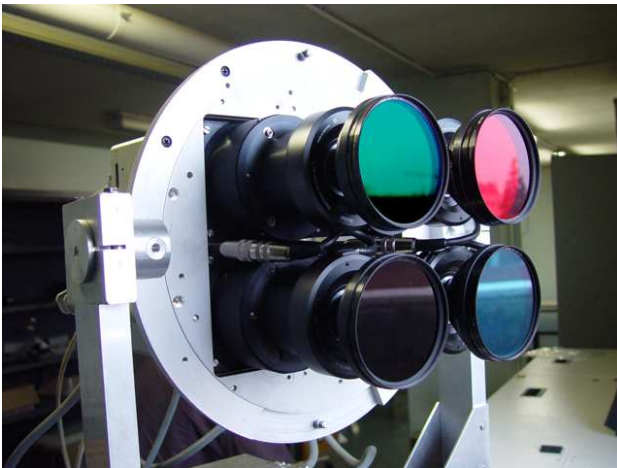


Figure 1. Four channels digital camera used in our study

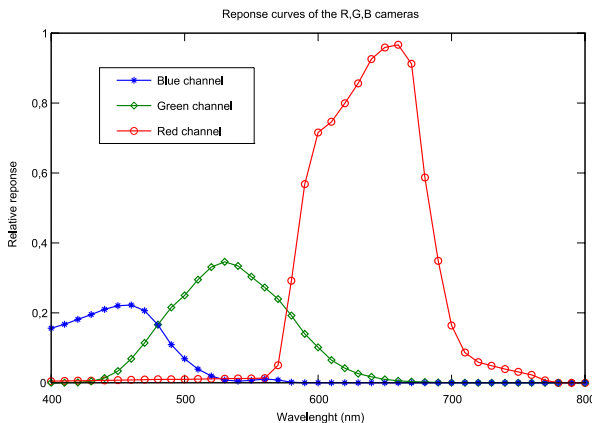


Figure 2. Cameras response for constant exposure and aperture

All the cameras are linked together by BNC connectors. This system provides a good synchronisation of the acquisition for the three R G B images that are superimposed to form a coloured image (Thom et al., 2001). In addition, the motion blur produced by the movement of the airplane (which is, in first order approximation, rectilinear and uniform) is corrected by Time Delayed Integration: the charge on each pixel are physically shifted in the sensor matrix in order to compensate the airplane's uniform movement knowing its elevation and speed. The device reaches a precision of half a pixel (CAMNU, 2005) and allows long exposure time acquisitions. However, it has some limits: the compensation is only made for a motion blur induced by the principal movement of the airplane and doesn't take into account perturbations such as drifts or rotations. They may cause a motion blur ranging from one to ten pixels in some images. Until now, an operator was in charge of visualising all the pictures one by one to sort out the blurred ones. In this production context, a tool automating this sorting would be highly beneficial.

3. STATE OF THE ART

Developments in Computer Science and the arrival of digital photography brought new hopes in the domain of image restoration. Even if blur kernel determination and blur correction appear as major topics in image processing, very few papers focus on blur detection.

A first description of blur can be done by considering the image edges. Such an approach is proposed by Tong who uses Haar wavelets to discriminate between blurred and sharp images (Tong et al., 2004). The method is independent from the blur kernel and the tests on our data have shown good results even on images with a small blur extension. Nevertheless, it is very sensitive to hot pixels (hardware flaw), which may cause too many false detections.

Another solution has been developed for partially blurred images (Liu et al., 2008) where different metrics are defined by considering some pieces of local information in spectral, spatial and colorimetric domain. Image regions are segmented into sharp, focus blurred and motion blurred classes by thresholding the different metrics. The parameters are chosen using a machine learning process. This method is local and thus not optimal for uniformly blurred images.

Other studies (Krahmer et al., 2006) suggest to use the notion of "cepstrum" defined by $C(s) = FT^{-1}(\log(|FT(s)|))$ where $FT(s)$ is the Fourier Transform of the signal s . In the case of motion blur that follows a rectangular function, its cepstrum shows two peaks, which distance and orientation gives information on the characteristics of the motion blur kernel. It provides acceptable results on images with a motion blur of large spread (more than 10 pixels), but is not at all adapted for our case where we want to sort out images with a motion blur of only one or two pixels.

The estimation of the blur kernel is often the major bottleneck in image restoration. This estimation may be performed through a probabilistic approach (Shan et al., 2008) and an iterative optimisation. This kind of method returns interesting results but its complexity makes it quite time consuming, which becomes somehow incompatible with the large number of images acquired during a single aerial mission. In addition, we are merely looking for a simple detector.

Contrary to the previous examples, other approaches (Lim et al. 2008, Yuan et al. 2007) do not limit themselves to a single image but exploit information from two images: one shot with a short exposure time (which provides a noisy image) and one with a long exposure time (which provides a motion blurred image). Even if this method is applied to image restoration, its concern is close to ours as motion blur estimation can be a means to achieve blur detection. During an aerial mission, a same spot is always seen on several pictures (on an average of four pictures), but the parallax resulting from the change of point of view makes this method inappropriate to our context.

Eventually, Raskar proposes a hardware solution (Raskar et al., 2006) using a coded exposure camera. The exposure is no longer a rectangular function but a succession of smaller rectangular functions of different temporal widths. This technique cannot be applied to the digital camera developed by the IGN because time exposure cannot currently be controlled below a certain threshold.

4. MONO-CHANNEL APPROACH

As the camera acquiring the blue channel has the longest exposure time, the images provided by this camera are more sensitive to motion blur than the ones provided by the other channels. Consequently, in this part, we focus on these blue channel images.

In the first place, some simplifying hypotheses should be stated in order to justify some choices made in our work:

- (H1). The blur kernel is a rectangular function centred on zero along a single direction. The exposure time is supposed to be short enough not to integrate non-uniform movements from the airplane. The fact that the centre of mass of the airplane does not correspond to the camera centre allows us to neglect rotation blurs that cannot be represented by a convolution (1).
- (H2). The cameras have a very good SNR, such that the noise may be neglected in our images.
- (H3). A sharp image can be considered as roughly isotropic, such that its Fourier Transform is also roughly isotropic: it has no preferred direction. The module of the Fourier Transform then also follows such a radial distribution.

The best way to represent a linear blur following hypotheses (H1) and (H2) is to consider the blurred image I_{blur} as a convolution of the sharp image I_{sharp} by a blur kernel f :

$$I_{blur} = I_{sharp} * f \quad (1)$$

Applying a Fourier Transform FT to the previous equation yields:

$$FT(I_{blur}) = FT(I_{sharp}) \times FT(f) \quad (2)$$

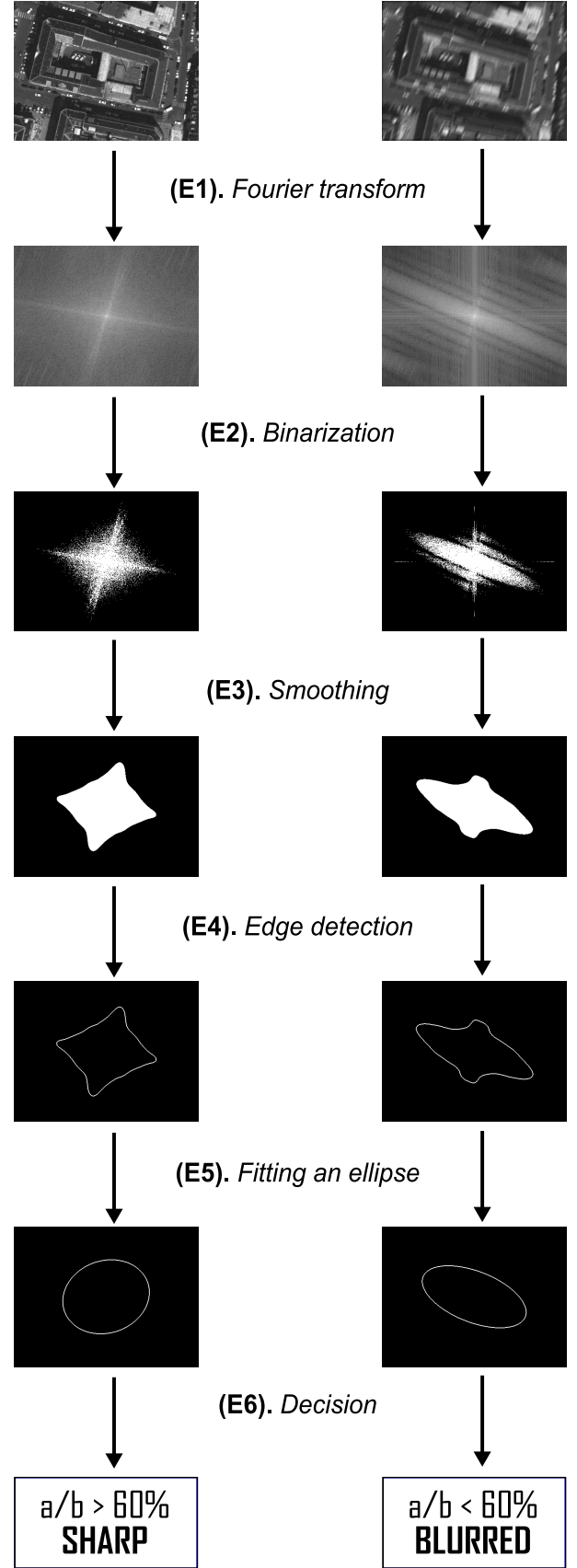


Figure 3. Our first approach for blur detection in aerial images

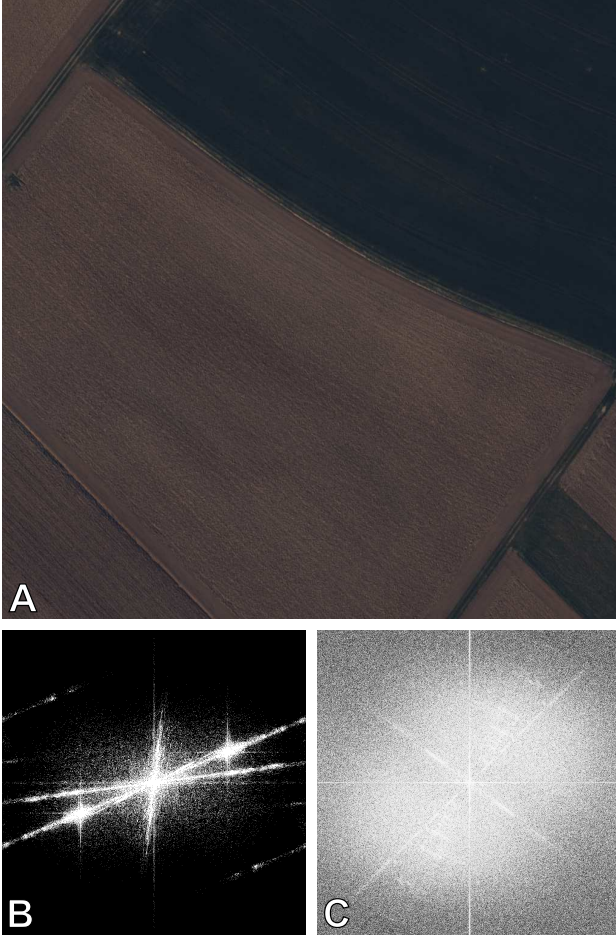


Figure 4. The sharp image (A) has an anisotropic Fourier Transform (B) which causes bad sorting with our initial mono-channel approach. Conversely, the difference of phase (6) is an isotropic signal (C) which will allow for a proper classification as not blurred.

In the case of images with motion blur, the high frequencies are cut down in a given direction and therefore the module of the Fourier Transform is not isotropic anymore. The proposed method to discriminate between sharp and blurred images is somehow intuitive and consist on looking whether the coefficients with high value module are concentrated preferentially in a circle (isotropic case) or in an ellipse (anisotropic case). This method could be divided into six steps that are summarized on Figure 3:

- (E1). Apply a Fourier Transform to the blue channel image.
- (E2). Binarize the module image by keeping only the 10% highest values. This statistic criterion is independent of the dynamic range of the image.
- (E3). Smooth this binary image by convolving it with a median filter to get rid of some artefacts such as the spikes caused by the periodic structures of the original image.
- (E4). Compute the edges of this binary image.
- (E5). Fit an ellipse to the edges by estimating its parameters θ (orientation), a (major axis) and b (minor axis).

- (E6). Sort between blurred and sharp images by thresholding the ratio a/b . We determined empirically that a threshold of 60% achieves the best compromise between under and over-detection.

This approach returns mostly good results but has its limits, especially when hypothesis (H3) is not respected. For example, images of ploughed fields are often detected as blurred but can be detected as sharp if they have a motion blur perpendicular to the furrows (Figure 4).

In order make our method more robust and in particular to get rid of hypothesis (H3), we propose the following approach that takes into account the channel-dependent specificity of our imaging system.

5. MULTI-CHANNELS APPROACH

Beforehand, let us replace hypothesis (H3) by:

- (H'3). The Fourier Transforms of the intensities of the three channels I^{blue} , I^{green} , I^{red} composing a sharp natural colour image have similar phases. According to (Oppenheim et al., 1981), the structure of an image is mostly held by the phase of its Fourier transform. This justifies this hypothesis as the three channels of a natural image have a common structure (in particular the same contours). If we call ϕ the phase of the Fourier Transform, this hypothesis writes:

$$\phi(I^{red}) \approx \phi(I^{green}) \approx \phi(I^{blue}) \quad (3)$$

Our idea is now to get rid of the possible natural anisotropy of our images (due to periodic structures present in urban areas or on ploughed fields) based on this property of natural images. It is somehow related to the idea of (Lim et al., 2008). The exposure time table shows that the red channel has the shortest exposure and therefore is the least affected by motion blur. Conversely, the blue channel has the longest exposure and is the most affected (Table 1). Thus we will now consider the red and blue channels separately:

$$\begin{aligned} I_{blur}^{red} &= I_{sharp}^{red} * f^{red} \\ I_{blur}^{blue} &= I_{sharp}^{blue} * f^{blue} \end{aligned} \quad (4)$$

If we take the difference of the phase of the Fourier transform of these two equations, we get:

$$\begin{aligned} \phi(I_{blur}^{red}) - \phi(I_{blur}^{blue}) &= \\ \phi(I_{sharp}^{red}) - \phi(I_{sharp}^{blue}) + \phi(f^{red}) - \phi(f^{blue}) \end{aligned} \quad (5)$$

Finally by applying (H'3) to the sharp image, we have:

$$\Delta\phi(I_{blur}) = \phi(I_{blur}^{red}) - \phi(I_{blur}^{blue}) \approx \phi(f^{red}) - \phi(f^{blue}) \quad (6)$$

This indicates that $\Delta\phi(I_{\text{blur}})$ depends much more on the blur characteristics than on the actual content of the images. Based on this remark, we propose a new multi-channel approach based by replacing steps (E2) of the mono-channel approach by the new steps (E'2):

- (E'2). Binarize the $|\Delta\phi(I_{\text{blur}})|$ image by thresholding the coefficients over $\pi/4$. The empirical choice of $\pi/4$ seems to make a good delimitation between the two areas where the frequencies are correlated or not (Figure 5). In case the phase is not defined, the pixel can be classified indifferently as these rare outliers will be removed by the smoothing (E3)

We also propose to modify the hard classification (E6) into the following three way classification (E'6):

- (E'6). Sort between blurred and sharp images by considering the same ratio a/b: if it is over 50%, the image will be classified as “sharp”, if it is less than 35%, the image will be classified as “blurred”, and if the ratio is between those two values, the image will be classified as “dubious”.

The third class “dubious” releases the classification process and provides a good confidence to “sharp” and “blurred” classification (Section 6). These thresholds have been chosen empirically on a representative set of 38 images.

6. VALIDATION OF THE MULTI-CHANNELS APPROACH

For the validation phase, the algorithm has been tested on a mission from April 2007, in rather poor conditions (low illumination). This mission is composed of 6271 pictures with various typologies (compact urban area, countryside, industrial area, forest...).

| | | HUMAN OPERATOR | | | |
|-----------|------------|-----------------|--------------|----------------|------------------|
| | | Sharp | Blurred | Unclassif | TOTAL |
| AUTOMATIC | Sharp | 1280 64,00 % | 0 0,00 % | 514 25,70 % | 1797 89,85 % |
| | Dubious | 25 1,25 % | 10 0,50 % | 48 2,40 % | 83 4,15 % |
| | Blurred | 1 0,05 % | 81 4,05 % | 32 1,60 % | 114 5,70 % |
| | Unclassif. | 0 0,00 % | 6 0,30 % | 0 0 % | 6 0,30 % |
| | TOTAL | 1309 65,45 % | 97 4,85 % | 594 29,70 % | 2000 100,00 % |

Table 2. Validation by a human operator

To validate our approach, a manual sorting has been completed by a human operator. The operator has sorted the images into two classes “sharp” and “blurred”. Some images were left “unclassified” by the operator. For instance, forest images are usually neglected to focus on inhabited areas, where the needs of ortho-images are stronger. For practical reasons, the validation concerned only a subset of 2000 images representative of the aerial mission. The images used for this validation were 1024x1024 crops taken at the centre of the

original 4096x4096 images where the optical quality is considered the best.

Even if Table 2 cannot be rigorously considered as a confusion matrix, it emphasizes the reliability of this method. Only one sharp image has been sorted as blurred by the computer and all the other blurred images have been well detected.

This method is semi automatic because the images from the “dubious” class should still be sorted by an operator. However, the computer has already made 95% of the work which saves a significant amount of time in production.

The whole validation process took around 11 hours (the code was not optimized). We also validated the choice of running the algorithm on centre crops by comparing the results with full size images on a smaller subset of 38 images. This resulted in the exact same classification for a division of the processing time by 16 between full images and crops, which justifies this choice operationally.

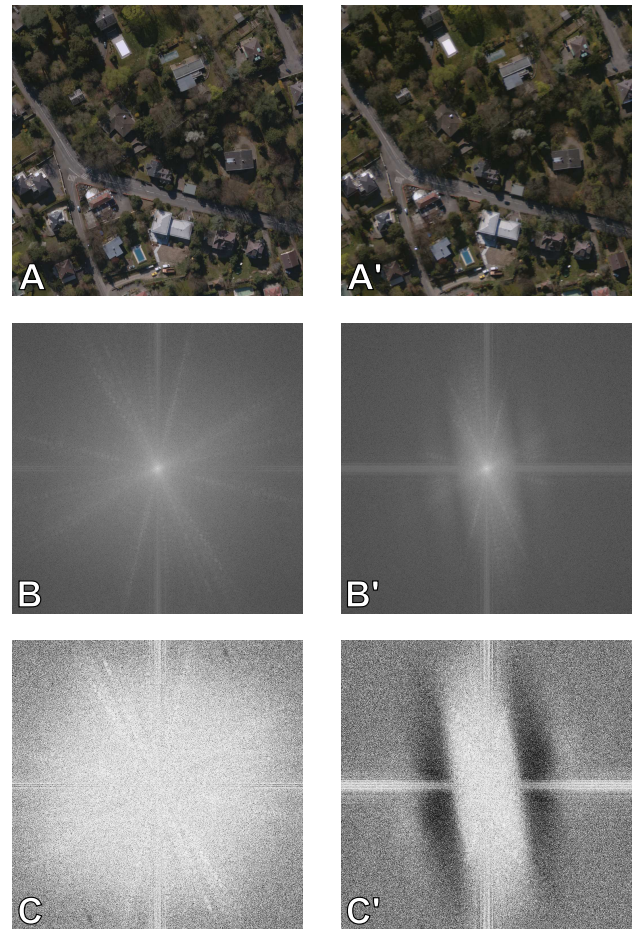


Figure 5. The images A and A' are crops of two successive images of an aerial mission focusing on the same area. Their respective Fourier Transforms are given by B and B'. The absolute value of the difference of phases (6) is displayed in C and C' with bright colours for low values and dark colour for value near π . The frequency peaks generated by urban structures have vanished.

7. CONCLUSIONS

This paper presents a simple method for motion blur detection in channel-dependent exposure time images, exploiting efficiently this specificity.

The main contribution of this paper is to leverage the multi-exposure sensing of the motion blur kernel, which undergoes an exposure-time linear scaling, whereas the phase differences between the underlying sharp colour channels are assumedly negligible.

The successful validation on 2000 aerial images will allow the use this technique in the operational context of a production chain.

In the future, the possibility of using the information provided by the difference (6) to estimate the blur kernel characteristics is a foreseeable lead. Eventually, this information could be used in order to restore the images detected as blurred.

ACKNOWLEDGEMENTS

The images are provided by the French National Mapping Agency's Image Database Department (IGN/SBI). The multi-channel camera technical characteristics are from the LOÉMI.

REFERENCES

- CAMNU, 2005; a description of IGN digital camera (accessed 28 May 2010): <http://recherche.ign.fr/LOEMI/AR/CAMNU/>
- Eastman Kodak Company, 2002, KAF-16801LE, 4096 (H) x 4096 (V) Pixel Enhanced Response Full-Frame CCD Image Sensor with Anti-Blooming Protection: Performance Specification, Revision 1.
- M. Kasser, Y. Egels, 2002, Generation of digital terrain and surface models, in *Digital Photogrammetry*, Taylor & Francis, London, UK, pp. 159-299.
- F. Krahmer, Y. Lin, B. McAdoo, K. Ott, J. Wang, D. Widemannk, 2006, Blind image deconvolution: motion blur estimation, Technical Report, Institute of Mathematics and its Applications, University of Minnesota.
- S. H. Lim, A. Silverstein, 2008, Estimation and Removal of Motion Blur by Capturing Two Images with Different Exposures, HP Labs Technical Reports, HPL-2008-170.
- R. Liu, Z. Li, J. Jia, 2008, Image Partial Blur Detection and Classification, *IEEE Conference on In Computer Vision and Pattern Recognition*, pp. 1-8.
- A.V. Oppenheim, J.S. Lim, 1981, The importance of phase in signals, *Proceedings of the IEEE*, vol. 69, n°5, pp. 529-541.
- R. Raskar, A. Agrawal, J. Tumblin, 2006, Coded Exposure Photography: Motion Deblurring Using Fluttered Shutter, *International Conference on Computer Graphics and Interactive Techniques*, ACM SIGGRAPH 2006 Papers, pp. 795-804.
- Q. Shan, J. Jia, A. Agarwala, 2008, High-quality Motion Deblurring from a Single Image, *ACM Transactions on Graphics*, vol. 27, n°3, Proceedings of ACM SIGGRAPH 2008, pp. 1-10.
- Ch. Thom, J.-Ph. Souchon, 2001, Multi-Head Digital Camera Systems, in *GIM International*, vol. 15, n°5, pp. 34-37.
- H. Tong, M. Li, H. Zhang, C. Zhang, 2004, *Blur detection for digital images using wavelet transform*. Proceedings of IEEE International Conference on Multimedia & Expo, pp. 17-20.
- L. Yuan, J. Sun, L. Quan, H.-Y. Shum, 2007, *Image deblurring with Blur-red/noisy image pairs*, International Conference on Computer Graphics and Interactive Techniques, ACM SIGGRAPH 2007 papers, vol. 26, n°3.